Analyst

PAPER

View Article Online
View Journal | View Issue

Cite this: *Analyst*, 2014, **139**, 1037

Nanostructured silver–gold bimetallic SERS substrates for selective identification of bacteria in human blood†

Arumugam Sivanesan,*[a] Evelin Witkowska,[a] Witold Adamkiewicz,[a] Łukasz Dziewit,[b] Agnieszka Kamińska*[a] and Jacek Waluk[a]

Received 11th October 2013
Accepted 5th December 2013

DOI: 10.1039/c3an01924a

www.rsc.org/analyst

Surface-enhanced Raman spectroscopy (SERS) is a potentially important tool in the rapid and accurate detection of pathogenic bacteria in biological fluids. However, for diagnostic application of this technique, it is necessary to develop a highly sensitive, stable, biocompatible and reproducible SERS-active substrate. In this work, we have developed a silver–gold bimetallic SERS surface by a simple potentiostatic electrodeposition of a thin gold layer on an electrochemically roughened nanoscopic silver substrate. The resultant substrate was very stable under atmospheric conditions and exhibited the strong Raman enhancement with the high reproducibility of the recorded SERS spectra of bacteria (*E. coli*, *S. enterica*, *S. epidermidis*, and *B. megaterium*). The coating of the antibiotic over the SERS substrate selectively captured bacteria from blood samples and also increased the Raman signal in contrast to the bare surface. Finally, we have utilized the antibiotic-coated hybrid surface to selectively identify different pathogenic bacteria, namely *E. coli*, *S. enterica* and *S. epidermidis* from blood samples.

1. Introduction

Progress of a modern society creates a rising demand for rapid diagnosis and discrimination of pathogenic bacteria, particularly in health care and clinical environments, food and water supplies, as well as in the fields of bioterrorism and bioengineering.[1–4] Numerous techniques, such as biochemical tests (API),[5] enzyme-linked immunosorbent assay (ELISA),[6] molecular biology,[7] and mass spectrometry,[4,8] have been developed for the detection or identification of bacteria. However, all of the above-mentioned methods have one or more shortcomings, including time-consuming analyses, complicated or expensive procedures, and often the need for highly trained personnel. Over the last decade, surface-enhanced Raman scattering spectroscopy (SERS) has turned out to be very promising in identifying bacteria at both the species and strain level by the "whole organism fingerprint" assessment.[9–11] The advantages of the SERS technique in bacterial identification are numerous: no need for cultivation, rapid diagnosis, easy handling, as well as the availability of compact and portable Raman spectrometers for direct field analysis.

The SERS technique exploits the enhancement of Raman scattering from molecules in close proximity to a nanostructured surface due to the coupling of metal surface plasmons with the oscillating electric field of the incident and scattered radiation.[12–14] An important aspect in SERS is the development of sensitive and stable SERS-active substrates. Most SERS studies of bacteria have been carried out using either silver colloids or roughened/nanostructured silver surfaces as SERS substrates.[10,11,15] Recently, a reproducible SERS-based platform capable of distinguishing different kinds of bacteria was reported using AgNPs grown on arrays of anodic aluminium oxide nanochannels.[16] However, two drawbacks to the use of silver are that it is toxic to bacteria[17] and that it is highly susceptible to surface oxidation, which leads to a decrease in SERS activity with time.[18] The use of gold nanoparticles (AuNPs) is promising since they are both biocompatible and highly stable with respect to oxidation.[19] In addition, AuNPs demonstrate very good optical properties, which has led to a growing body of literature showing the development of AuNP-based SERS substrates for bacterial identification.[19–25]

Some of the latest works successfully employed bimetallic nanoparticles as SERS substrates with higher signal enhancement and biocompatibility than the monometallic AgNPs.[26–33] Bimetallic nanoparticles consistently exhibit higher SERS enhancement than monometallic nanoparticles. It has also been shown that it can be advantageous to coat a SERS surface with an antibiotic to improve selectivity and enhance capturing.[34] Here, we focus on combining these principles with two objectives: (a) simple fabrication and characterization of a

[a]*Institute of Physical Chemistry, Polish Academy of Sciences, Kasprzaka 44/52 01-224 Warsaw, Poland. E-mail: asnesan@gmail.com; akamin@ichf.edu.pl; Tel: +48 22 343 32 28*

[b]*University of Warsaw, Faculty of Biology, Institute of Microbiology, Department of Bacterial Genetics, Miecznikowa 1, 02-096 Warsaw, Poland*

† Electronic supplementary information (ESI) available. See DOI: 10.1039/c3an01924a

highly sensitive and stable silver–gold (Ag–Au) bimetallic SERS substrate and (b) utilization of the substrate for selective identification of bacteria in human blood. The new SERS substrate was produced using potentiostatic electrodeposition of a thin gold layer on an electrochemically roughened nanoscopic silver substrate. Vancomycin and ceftazidime hydrate were tested on the bimetallic surface as a first step in assessing the ability of different antibiotics to increase the selectivity and capturing of pathogenic bacteria from human blood on the new type of SERS-active surface.

2. Experimental section

2.1. Chemicals and materials

Hydrogen tetrachloroaurate(III) hydrate, vancomycin, ceftazidime hydrate, perchloric acid, and potassium chloride were purchased from Sigma-Aldrich. Polishing slurries and pads (Microcloth®) were purchased from Buehler, Germany. The chemicals were used without any further purification. A polycrystalline silver disc electrode having a geometric area of 0.785 cm^2 and a platinum wire (Mennica Metale Szlachetne, Warsaw, Poland) were used as the working and counter electrode, respectively. Leakless Ag/AgCl electrode (eDAQ Europe) was used as a reference electrode. The electrochemical experiments were performed in a custom-made three-electrode cell setup.

All bacterial species (*Escherichia coli*, *Salmonella enterica*, *Staphylococcus epidermidis* and *Bacillus megaterium*) used in the experiment were obtained from the Department of Bacterial Genetics, University of Warsaw, Poland.

2.2. Instrumentation

Electrochemical experiments were carried out in a μAutolab potentiostat (Metrohm Autolab). SERS measurements were performed using the Renishaw inVia Raman system equipped with a 300 mW diode laser emitting a 785 nm line which was used as an excitation source. The laser light was passed through a line filter and focused on a sample mounted on an *X–Y–Z* translation stage with a 50× objective lens (numerical aperture 0.75) that focused the laser to a spot size of around 2.5 μm. The Raman-scattered light was collected by the same objective through a holographic notch filter to block the Rayleigh scattering. A 1200 grooves per mm grating was used to provide a spectral resolution of 5 cm^{-1}. The Raman scattering signal was recorded by a 1024 × 256 pixel RenCam CCD detector. Typically, the spectra were acquired for 4 s, with 5 mW of the laser power measured at the sample. SERS mapping was carried out by randomly selecting 5 mapping areas over the entire substrate. Mapping was performed in an area of 1000 μm^2. 30 spectra were collected from each mapping region. In total 150 spectra were collected for each sample and averaged.

SEM measurements were performed using a FEI Nova™ NanoSEM 450 scanning electron microscope with an accelerating voltage of 10 kV under high vacuum. XPS measurements were carried out in a PHI 5000 VersaProbe™ – Scanning ESCA Microprobe™ (ULVAC-PHI, Japan/USA, 2008) instrument at base pressure $<5 \times 10^{-9}$ mbar. Monochromatic Al K_α radiation was used and the X-ray beam, focused to a 100 μm diameter, was scanned over a (250 × 250) μm^2 surface at an operating power of 25 W (15 kV).

2.3. SERS substrate preparation

Preparation of the rough silver substrate. Silver disc electrodes were mechanically mirror-polished with alumina slurries with sequentially decreasing particle sizes (0.5 μm, 0.05 μm and 0.02 μm). After each step of polishing, the electrodes were immersed in Millipore water and subsequently sonicated in an aqueous ultrasonic bath for 15 minutes to remove the physically adsorbed alumina particles from the electrode surface. After polishing, the electrodes were electrochemically roughened with an oxidation/reduction cycle (ORC). The electrochemical cell was filled with 0.1 M KCl solution and subsequently purged with argon gas for 30 min to remove most of the oxygen from the solution. The rough silver substrate was prepared by three ORCs (0.5 V for 40 s and −0.5 for 40 s; 0.5 V for 15 s and −0.5 for 15 s and in the end, 0.5 V for 15 s and −0.5 for 30 s) and a final reduction potential of −0.4 V for 300 s. The electrode was then thoroughly washed with Millipore water and dried with a flow of argon gas.

Preparation of the silver–gold bimetallic surface. The silver–gold bimetallic surface was prepared by electrochemical deposition of nanostructured gold over an electrochemically roughened silver surface. The three-electrode electrochemical cell was filled with the solution of 0.4 mM $HAuCl_4$ in 0.1 M $HClO_4$ and subsequently purged with argon gas for 30 min to remove most of the oxygen from the solution. A potential of −80 mV was applied for 200 s and then the electrode was removed from the solution and subsequently washed with Millipore water to remove other ions from the surface. The electrode was then dried with a flow of argon gas and used as a SERS substrate.

Antibiotic-coating on the SERS substrate. The antibiotic-coated hybrid SERS substrate was prepared by immersing the dried Ag–Au bimetallic substrate in a 10 mM aqueous solution of vancomycin or ceftazidime hydrate for 1 h. The coated substrate was subsequently dried overnight in air.

2.4. Bacteria culture and SERS sample preparation

To multiply microbial organisms, they were cultivated in the liquid LB (Lysogeny broth) growth medium, and then incubated in a shaker (150 rpm) at 30 °C for 24 h. Afterwards, the bacteria were dispersed in Millipore water and centrifuged for 10 min at 4000 rpm in order not to destroy the cell membrane. Finally, the supernatant liquid was discarded and the bacterial cells were redispersed in Millipore water. The centrifugation process was repeated 5 times to obtain a solution of clean bacterial cells. The purified bacteria were dispersed in Millipore water to a clinically significant concentration of 10^2 CFU mL^{-1}. The density of bacterial cells was determined by counting the number of colonies grown on a Petri dish, starting from a known amount of the medium. The count was taken after one day of cultivation at 37 °C. About 50 μL of aqueous bacterial solution was applied to the SERS substrate, both with and without antibiotic coating, and incubated at 30 °C for 1 h. The sample was washed with

Millipore water and dried in a flow of argon gas before using for Raman and SEM measurements.

3. Results and discussion

3.1. Characterization of the bimetallic surface

In producing a highly active Ag–Au SERS substrate, both the distance of deposited Au particles from the silver base[28] and the morphology of the surface[35,36] are important. Because of this, experiments were performed with varying parameters such as the concentration of electrolytes, the value of the reduction potential and the time for which it was applied, as well as the concentration of $HAuCl_4$ which was the source of deposited gold. The morphology of rough silver surfaces and silver–gold bimetallic surfaces produced using optimal conditions was studied by SEM imaging. The results are shown in Fig. 1. The SEM image of the rough silver surface (Fig. 1a) reveals a nanoporous structure with the grain size ranging from 30 to 200 nm. The SEM image of the silver–gold bimetallic surface (Fig. 1c) shows, in contrast to the rough silver surface, a more uniform nanostructure with less porosity and increased grain size. Viewed over a wider scanning area (Fig. 1b), the substrate is homogeneous, unlike substrates prepared from colloids, and therefore should produce analogous spectra for the same bacterial species in any substrate location. The closer view of the bimetallic surface depicts a crystalline structure for the deposited gold layer (Fig. 1d).

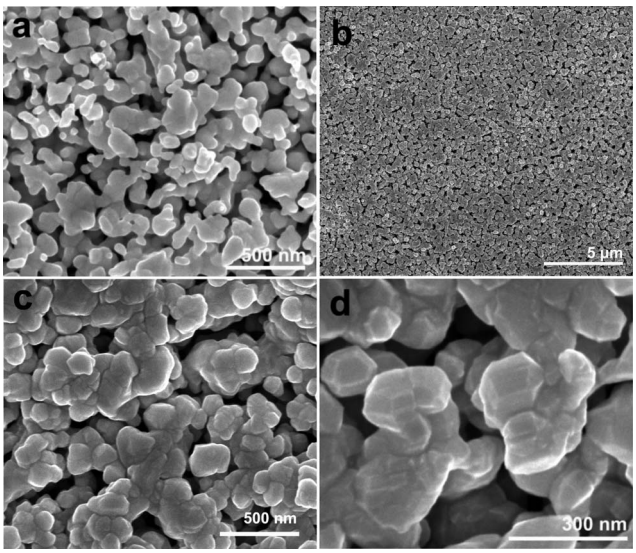

Fig. 1 SEM images of the (a) rough silver surface and (b–d) silver–gold bimetallic surface at different magnifications.

The Au deposition was further investigated using X-ray photoelectron spectroscopy (XPS) (Fig. 2). For a Ag $3d_{5/2}$ electron in a pure silver surface, a binding energy of 368.2 eV was obtained. In comparison, a Ag $3d_{5/2}$ electron in a Ag–Au surface gives a binding energy of 368.0 eV. The same difference was obtained for a Ag $3d_{3/2}$ electron. This compares well with previous measurements.[37,38] Gold behaves in a similar fashion. It has also been shown that a Au $4f_{7/2}$ electron in bulk metallic gold has a binding energy of 84 eV. In comparison to bulk gold, the binding energy for a Au $4f_{7/2}$ electron in the Ag–Au surface is 83.8 eV. For both silver and gold in a bimetallic surface, the

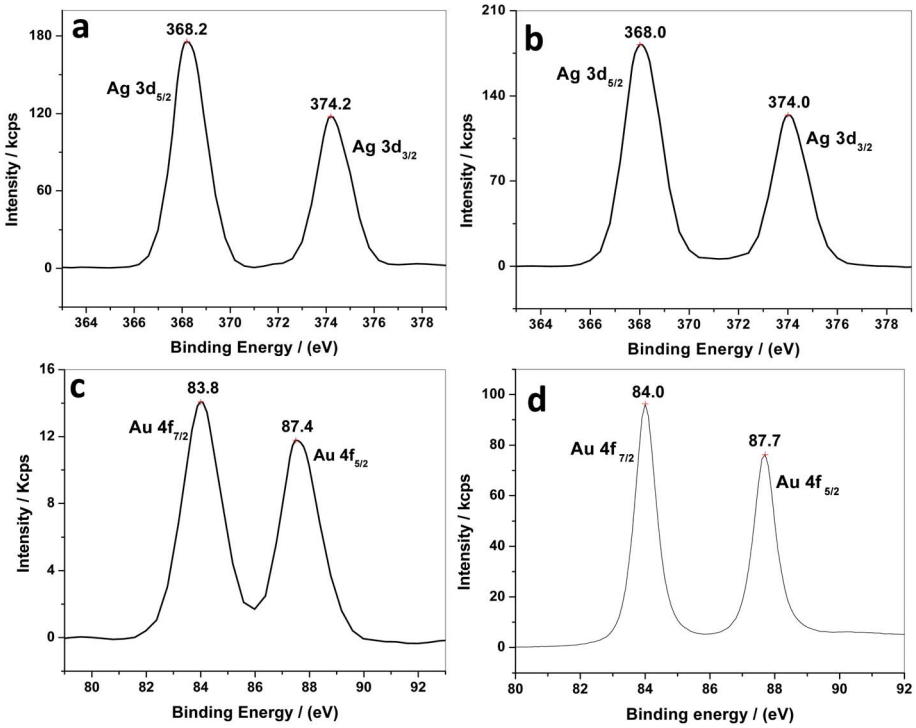

Fig. 2 XPS data of (a) Ag 3d for silver, (b) Ag 3d for Ag–Au bimetallic surface, (c) Au 4f for Ag–Au bimetallic surface, and (d) Au 4f for gold.

binding energy is lower than in the pure bulk metal.[38] Using intensity data for Au $4f_{7/2}$ and Ag $3d_{5/2}$ electrons (Fig. 2), the percentage of Au and Ag in the bimetallic surface can be estimated to be 7.6 and 87.4, respectively, assuming the same cross-section for the bulk and bimetallic surface. The remaining 5 percent can be attributed to chlorine and oxygen. The estimated low percentage of Au in the bimetallic surface confirms that it forms a thin layer on the Ag base.

3.2. Stability and reproducibility of the bimetallic SERS substrate

The stability of the SERS substrate is very important for practical application to fingerprinting bacteria. The stability of the silver–gold bimetallic substrates was tested by exposing them to air and then performing SERS experiments on bacteria using the procedure previously described in the Experimental section. Four bimetallic SERS substrates were tested, following the exposure to air for 1, 5, 10 and 15 days, as well as one which was freshly produced. For *S. epidermidis*, SERS mapping was performed. For each substrate an average spectrum was produced from 150 individual spectra. All five substrates showed similar spectra. Using the band at 731 cm^{-1} as a reference, the intensity from each of the 5 substrates was compared (Fig. S1A†). The standard deviation of the intensity of the 731 cm^{-1} peak was around 15% for the 150 spectra collected at different locations on the same substrate. There is no relationship between the SERS signal and the time of exposure to air. This clearly confirms that the silver–gold bimetallic substrate is very stable under atmospheric conditions. The reproducibility of the bimetallic substrate was tested by adsorbing *S. epidermidis* on 5 different bimetallic SERS substrates prepared under identical conditions (Fig. S1B†). Considering the 731 cm^{-1} band as the reference, the standard deviation was found to be 17% among different substrates and this is still a good number for SERS.

3.3. Bacteria on bimetallic and pure silver surfaces

In order to determine how the bare bimetallic surface enhances the SERS signal in comparison with a bare silver surface, both substrates were coated with equal concentrations of *S. epidermidis* and SERS spectra were recorded (Fig. S2†). The SERS spectra of bacterial species on the bimetallic surface show higher signal intensity and lower background than for the rough silver surface. In addition, the two bands at 1569 cm^{-1} and 1636 cm^{-1} are clearly distinguishable on the bimetallic surface, while on the rough silver surface they are merged and appear broadened. The improvement in spectral resolution is beneficial for spectral fingerprinting which relies on high signal intensity and peak resolution for successful use.

The highest Raman signal enhancement appears when there is a combination of surface and resonance effects. The maximum resonance effect is expected when the λ_{max} of the substrate surface plasmon resonance (SPR) is located in-between the exciting (785 nm for this experiment) and Raman-scattered wavelengths (here at 833 nm, corresponding to the 731 cm^{-1} band).[39] In general, the SPR maximum of silver nanostructures is located in the range of 400–500 nm, but when a layer of gold is deposited over a nanostructured silver surface the SPR is anticipated to red shift.[40] Better match between the excitation wavelength and SPR should result in a higher enhancement.

3.4. SERS investigation of bacteria on the bare and antibiotic-coated hybrid substrate

Gram-positive (*B. megaterium* and *S. epidermidis*) and Gram-negative (*E. coli* and *S. enterica*) bacteria were deposited on both antibiotic-coated and bare SERS substrates at a concentration of 10^2 CFU mL^{-1}. Fig. 3 shows the SERS spectra of these species on both antibiotic-coated and bare Ag–Au bimetallic surfaces in the information-rich part of the spectrum between 600 and 1700 cm^{-1}. The SERS signals of bacteria are derived from their cell wall components. All tested bacterial species show common intense spectral features around 731 cm^{-1} and 1330 cm^{-1}. These are related to the adenine part of the flavin derivatives or glycosidic ring mode of the polysaccharides.[9,41,42] The band positions of *E. coli* bacteria tested and their corresponding assignments are in agreement with the literature values.[9] Apart from these two important bands, all bacterial species reveal their own individual spectral characteristics which aid in the whole organism fingerprint analysis. For example, the band at 655 cm^{-1} can be seen in *E. coli* and *B. megaterium*, but not in *S. enterica* or *S. epidermidis*. To distinguish between *E. coli* and *B. megaterium* the ratio of intensities of the peaks at 655 cm^{-1} and 731 cm^{-1} can be used. *S. enterica* and *S. epidermidis* can be

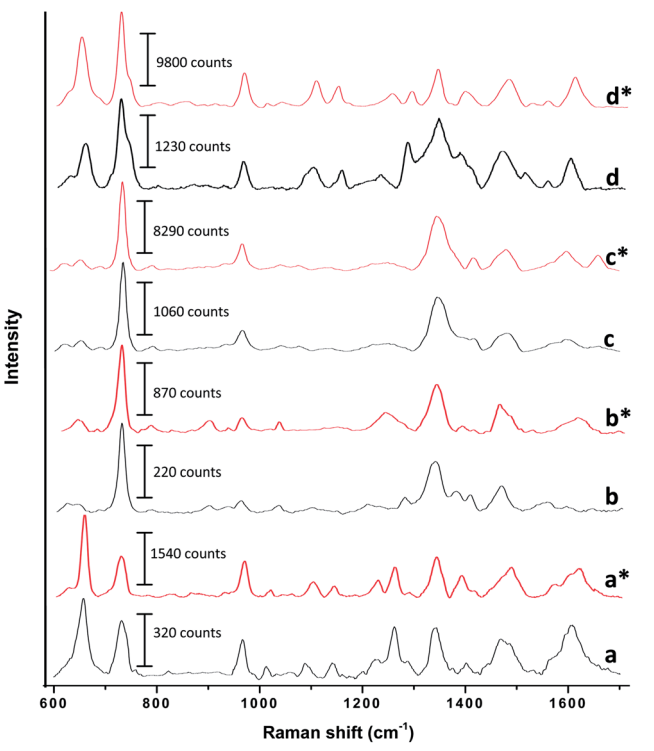

Fig. 3 SERS spectra of (a) *E. coli*, (b) *S. enterica*, (c) *S. epidermidis* and (d) *B. megaterium* on the bare Ag–Au bimetallic surface. The spectra labeled a*–d* represent the corresponding bacteria on a vancomycin-coated Ag–Au hybrid surface.

distinguished from the others using bands at 891 cm^{-1} for *S. enterica* and 1595 cm^{-1} and 1660 cm^{-1} for *S. epidermidis*.

Antibiotics are agents that inhibit bacterial growth or kill bacteria. They are commonly classified based on their mechanism of action, chemical structure, or spectrum of activity. Some of them can act by inhibiting proper cell wall synthesis. To do this, the antibiotic must bind to the peptidoglycan (Gram-positive) or lipopolysaccharide (Gram-negative) layer of the bacterial cell wall. When the SERS substrate is coated with the antibiotic, this interaction also increases the trapping of bacteria.[34] This principle has been applied in the present study to enhance the bacteria capturing ability of SERS substrates to enhance the SERS signal.

Two antibiotics, vancomycin and ceftazidime hydrate, were tested for their bacteria capturing ability with four different species of bacteria: *E. coli*, *S. enterica*, *S. epidermidis* and *B. megaterium*. Vancomycin is an antibiotic effective against Gram-positive bacteria and ceftazidime hydrate is effective against Gram-negative bacteria. The use of either antibiotic resulted in stronger bacterial SERS signals on the hybrid substrate than when no antibiotic was used. However, vancomycin showed better SERS enhancement than ceftazidime hydrate for all bacterial species irrespective of whether they were Gram-positive or Gram-negative. Furthermore, the SERS spectrum of vancomycin itself seems simple and broadened, in contrast to ceftazidime hydrate (Fig. S3†). A detailed SERS study using a wide range of antibiotics to assess the feasibility of Gram-selective bacteria capturing is still in progress[43] but for now, vancomycin is preferred in the present study.

Fig. 3 compares the SERS spectra of four bacterial species obtained on a vancomycin-coated hybrid surface and on an uncoated bimetallic surface. The position and shape of all bacterial vibrational bands on the vancomycin-coated substrate are similar to those of the bare bimetallic substrate, except for a small change in the shape of a few bands, which shows that vancomycin does not significantly interfere with the SERS spectrum of bacteria. Furthermore it is worth mentioning that the intensity of SERS signals from the vancomycin-coated substrate in comparison with the bare substrate is ~8 times higher for *S. epidermidis* and *B. megaterium*, ~4 times higher for *S. enterica* and ~5 times for *E. coli*. The reason of higher signal intensity for *S. epidermidis* and *B. megaterium* than for *E. coli* and *S. enterica* is that vancomycin is more effective against Gram-positive than Gram-negative bacteria.

To confirm that bacteria are in fact immobilized on the surface, SEM measurements were performed for bacteria on the bare and vancomycin-coated hybrid surface (Fig. 4). Although *B. megaterium* is not found in blood, it was used for the SEM measurements since it is readily available and easily distinguished in images. Fig. 4 shows *B. megaterium* immobilized on the substrate. The SEM images of *E. coli*, *S. enterica*, and *S. epidermidis* are shown in Fig. S4.† The condition of the cell wall for bacteria can vary and is prone to manipulation and exposure to vacuum necessary for making SEM measurements in the absence of any protective agent. The effect of vancomycin in trapping is most clearly seen in contrasting the SEM images for coated and non-coated substrates which have been treated with

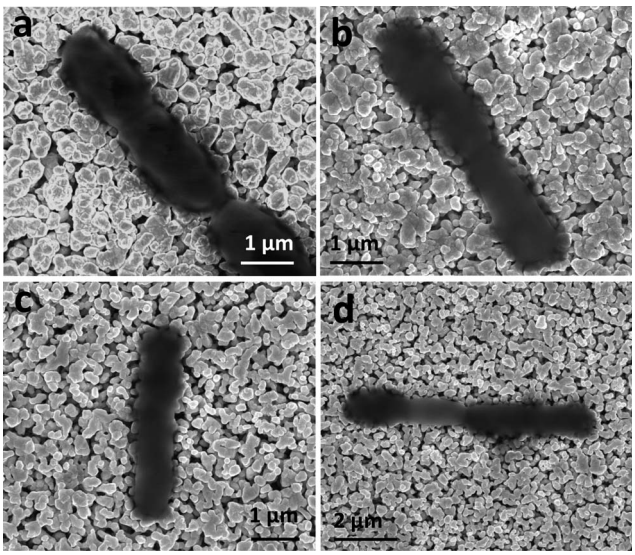

Fig. 4 SEM images of *B. megaterium* on the (a) bare bimetallic and (b–d) vancomycin-coated Ag–Au hybrid surface.

bacteria, followed by strong flushing with water and drying with inert gas. The number of bacteria on samples not coated with vancomycin was ~95% lower than for vancomycin-coated substrates because of the fact that bacteria on uncoated samples were simply flushed away. This experiment provides a positive sign that the antibiotic-coated SERS substrate could be used for bacterial identification in body fluids in such a way that other biological contaminants could be washed away, leaving behind bacterial marker on the substrate.

3.5. Identification of bacteria in human blood

To test the ability of vancomycin-coated Ag–Au hybrid SERS substrates to retrieve bacteria from human blood samples, selected healthy human blood samples were injected with bacteria contained in physiological solution. Fig. 5a shows the SERS spectrum of *S. epidermidis* from a blood sample injected with bacteria. It is in complete agreement with the previous SERS spectrum of *S. epidermidis* from an aqueous medium. In addition, the SERS spectrum of a healthy blood sample in the absence of bacteria does not show any significant bands. This confirms that the vancomycin-coated Ag–Au SERS substrate does not capture or bind blood components. This observation was further verified using SEM for *S. epidermidis* (Fig. 5b), which also shows no evidence of retained blood components. Similar results were obtained for blood samples spiked with *E. coli* and *S. enterica*.

In conclusion, we have developed a new, stable Ag–Au bimetallic SERS substrate with better SERS enhancement than the usual rough silver surface. An antibiotic coating of vancomycin on the SERS substrate enhances capturing of bacteria, but does not retain human blood components. Already at this stage the method shows promise for application in a clinical setting. The present vancomycin-coated Ag–Au substrate is a promising platform for practical identification of bacteria in

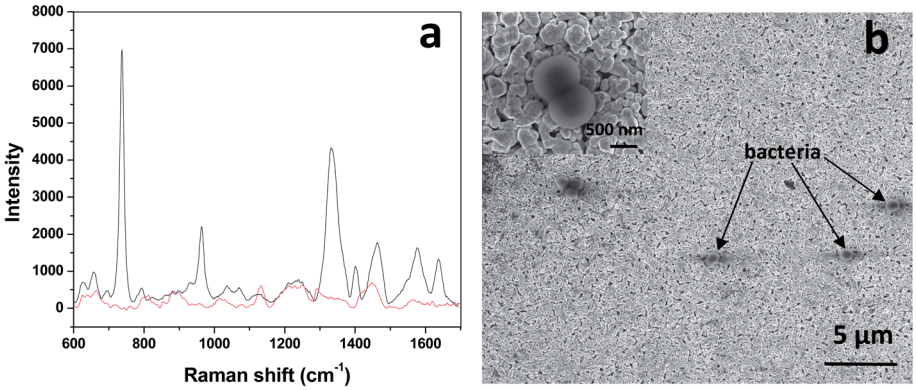

Fig. 5 (a) SERS spectra of healthy human blood (red) and *S. epidermidis* spiked human blood (black) on the vancomycin-coated Ag–Au hybrid surface. (b) SEM image of *S. epidermidis* selectively captured from blood components on a vancomycin-coated Ag–Au hybrid substrate. The inset shows the close view of *S. epidermidis*.

real body fluids. Nevertheless, a great deal of work remains in creating a bacterial SERS database to make such measurements more universally applicable in a variety of fields.

Acknowledgements

We would like to thank Wojciech Lisowski and Janusz Sobczak from the Institute of Physical Chemistry PAN for XPS measurements shown in this paper. The research was supported by the Foundation for Polish Science – POMOST Programme co-financed by the European Union within European Regional Development Fund. SEM FEI NovaNano 450 system and Arumugam Sivanesan's work were financed by the EC 7.FP under the Research Potential (Coordination and Support Actions FP7-REGPOT-CT-2011-285949-NOBLESSE).

References

1 H. J. R. Stevenson and O. E. A. Bolduan, *Science*, 1952, **116**, 111–113.
2 R. I. Amann, W. Ludwig and K. H. Schleifer, *Microbiol. Rev.*, 1995, **59**, 143–169.
3 M. Zourob, S. Elwary and A. Turner, *Principles of Bacterial Detection: Biosensors, Recognition Receptors and Microsystems*, Springer, 233 Spring Street, New York, NY 10013, USA, 2008.
4 S. Sauer and M. Kliem, *Nat. Rev. Microbiol.*, 2010, **8**, 74–82.
5 D. A. B. Dance, V. Wuthiekanun, P. Naigowit and N. J. White, *J. Clin. Pathol.*, 1989, **42**, 645–648.
6 N. Yahaya, S. Kaspan, N. R. Abdullah and S. Pit, *Int. Med. J.*, 2007, **14**, 243–246.
7 T. Matsuki, K. Watanabe and R. Tanaka, *Curr. Issues Intest. Microbiol.*, 2003, **4**, 61–69.
8 E. Carbonnelle, C. Mesquita, E. Bille, N. Day, B. Dauphin, J.-L. Beretti, A. Ferroni, L. Gutmann and X. Nassif, *Clin. Biochem.*, 2011, **44**, 104–109.
9 A. Walter, A. Marz, W. Schumacher, P. Rosch and J. Popp, *Lab Chip*, 2011, **11**, 1013–1021.
10 S. Efrima and L. Zeiri, *J. Raman Spectrosc.*, 2009, **40**, 277–288.
11 R. M. Jarvis and R. Goodacre, *Chem. Soc. Rev.*, 2008, **37**, 931–936.
12 M. Moskovits, *Rev. Mod. Phys.*, 1985, **57**, 783–826.
13 A. Otto, I. Mrozek, H. Grabhorn and W. Akemann, *J. Phys.: Condens. Matter*, 1992, **4**, 1143–1212.
14 Z.-Q. Tian, B. Ren and D.-Y. Wu, *J. Phys. Chem. B*, 2002, **106**, 9463–9483.
15 R. A. Tripp, R. A. Dluhy and Y. Zhao, *Nano Today*, 2008, **3**, 31–37.
16 T. Y. Liu, Y. Chen, H. H. Wang, Y. L. Huang, Y. C. Chao, K. T. Tsai, W. C. Cheng, C. Y. Chuang, Y. H. Tsai, C. Y. Huang, D. W. Wang, C. H. Lin, J. K. Wang and Y. L. Wang, *J. Nanosci. Nanotechnol.*, 2012, **12**, 5004–5008.
17 Z.-M. Xiu, Q.-B. Zhang, H. L. Puppala, V. L. Colvin and P. J. J. Alvarez, *Nano Lett.*, 2012, **12**, 4271–4275.
18 H. Li and B. M. Cullum, *Appl. Spectrosc.*, 2005, **59**, 410–417.
19 H.-W. Cheng, S.-Y. Huan and R.-Q. Yu, *Analyst*, 2012, **137**, 3601–3608.
20 W. R. Premasiri, D. T. Moir, M. S. Klempner, N. Krieger, G. Jones and L. D. Ziegler, *J. Phys. Chem. B*, 2004, **109**, 312–320.
21 R. M. Jarvis, N. Law, I. T. Shadi, P. O'Brien, J. R. Lloyd and R. Goodacre, *Anal. Chem.*, 2008, **80**, 6741–6746.
22 P.-J. Huang, L.-L. Tay, J. Tanha, S. Ryan and L.-K. Chau, *Chem. – Eur. J.*, 2009, **15**, 9330–9334.
23 B. Yan, A. Thubagere, W. R. Premasiri, L. D. Ziegler, L. Dal Negro and B. M. Reinhard, *ACS Nano*, 2009, **3**, 1190–1202.
24 H.-W. Cheng, S.-Y. Huan, H.-L. Wu, G.-L. Shen and R.-Q. Yu, *Anal. Chem.*, 2009, **81**, 9902–9912.
25 H.-W. Cheng, Y.-Y. Chen, X.-X. Lin, S.-Y. Huan, H.-L. Wu, G.-L. Shen and R.-Q. Yu, *Anal. Chim. Acta*, 2011, **707**, 155–163.
26 M. Mandal, S. Kundu, S. K. Ghosh, N. R. Jana, M. Panigrahi and T. Pal, *Curr. Sci.*, 2004, **86**, 556–559.
27 J. D. Driskell, R. J. Lipert and M. D. Porter, *J. Phys. Chem. B*, 2006, **110**, 17444–17451.
28 Z.-Q. Tian, B. Ren, J.-F. Li and Z.-L. Yang, *Chem. Commun.*, 2007, 3514–3534.
29 Y. Yang, J. Shi, G. Kawamura and M. Nogami, *Scr. Mater.*, 2008, **58**, 862–865.

30 J. J. Feng, U. Gernert, M. Sezer, U. Kuhlmann, D. H. Murgida, C. David, M. Richter, A. Knorr, P. Hildebrandt and I. M. Weidinger, *Nano Lett.*, 2009, **9**, 298–303.
31 Y. Cui, B. Ren, J. L. Yao, R. A. Gu and Z. Q. Tian, *J. Phys. Chem. B*, 2006, **110**, 4002–4006.
32 P. Wu, Y. Gao, H. Zhang and C. Cai, *Anal. Chem.*, 2012, **84**, 7692–7699.
33 M. Fan, F.-J. Lai, H.-L. Chou, W.-T. Lu, B.-J. Hwang and A. G. Brolo, *Chem. Sci.*, 2013, **4**, 509–515.
34 T. Y. Liu, K. T. Tsai, H. H. Wang, Y. Chen, Y. H. Chen, Y. C. Chao, H. H. Chang, C. H. Lin, J. K. Wang and Y. L. Wang, *Nat. Commun.*, 2011, **2**, 538.
35 A. G. Brolo, D. E. Irish, G. Szymanski and J. Lipkowski, *Langmuir*, 1998, **14**, 517–527.
36 G. V. P. Kumar, *J. Nanophotonics*, 2012, **6**, 064503.
37 D. Oyamatsu, M. Nishizawa, S. Kuwabata and H. Yoneyama, *Langmuir*, 1998, **14**, 3298–3302.
38 A. Q. Wang, J. H. Liu, S. D. Lin, T. S. Lin and C. Y. Mou, *J. Catal.*, 2005, **233**, 186–197.
39 A. D. McFarland, M. A. Young, J. A. Dieringer and R. P. Van Duyne, *J. Phys. Chem. B*, 2005, **109**, 11279–11285.
40 M. J. Beliatis, S. J. Henley and S. R. P. Silva, *Opt. Lett.*, 2011, **36**, 1362–1364.
41 L. Zeiri, B. V. Bronk, Y. Shabtai, J. Eichler and S. Efrima, *Appl. Spectrosc.*, 2004, **58**, 33–40.
42 M. Kahraman, M. M. Yazici, F. Sahin and M. Culha, *Langmuir*, 2008, **24**, 894–901.
43 T.-T. Liu, Y.-H. Lin, C.-S. Hung, T.-J. Liu, Y. Chen, Y.-C. Huang, T.-H. Tsai, H.-H. Wang, D.-W. Wang, J.-K. Wang, Y.-L. Wang and C.-H. Lin, *PLoS One*, 2009, **4**, e5470.